

HEAT TRANSFER IN A PHOSPHORIC ACID FUEL CELL STACK

Taeyeon Hwang, Jongheop Yi and Hwayong Kim[†]

Department of Chemical Engineering, Seoul National University, Seoul 151-742, Korea

(Received 19 September 1993 • accepted 9 September 1994)

Abstract—The electricity production in PAFC (Phosphoric Acid Fuel Cell) is accompanied by approximately equal amount of heat generation. For the best performance and efficient operation of the fuel cell stack, temperature distribution in the fuel cell stack should be controlled. Because the temperature gradient, both in the direction of stacking and in the cell plate, affects the cell performance, endurance, electrolyte loss, and corrosion. In this study, a 30-plate phosphoric acid fuel cell stack was analyzed and modelled by using electrochemical equations and heat and mass transfer equations. To obtain more realistic profiles, local values of temperature and current density were used in the calculation. Obtained results agreed well with experimentally measured values: the temperature deviation from the measured values was less than 1.5°C.

Key words: *Phosphoric Acid Fuel Cell, Stack Simulation, DIGAS Cooling System, Temperature Distribution, Current Density Profile*

INTRODUCTION

A fuel cell is a device that directly converts the chemical energy of reactants (a fuel and an oxidant) into electricity by catalytic reactions. This has many merits such as high efficiency of energy conversion, capability of using alternative fuels including natural gases and methanol, few creations of environmental pollution [1]. Furthermore, construction time is relatively shorter than that of conventional power plants and construction area is smaller. So it is possible to be constructed anywhere it is needed [2].

The principles of fuel cell operation were explained by Grove and it is named fuel cell by Ludwig and Charles Langer in 1889. It was W. Nernst and R. Haber who built and analyzed the principle of the Carbon-oxidizing fuel cell. Schmid developed the gas-diffusion electrode in 1920s. Later 5KW power plant was built by Bacon and after 1960s it was put into practical use as the source of electric power and drinking water in the aero space project like Apollo and Gemini project [3].

The fuel cells can be classified into several types by the electrolyte used and operation temperature. Among these, the most practical one is PAFC. Performance test of a low pressure and low temperature type fuel cell as a substitutive system of thermoelectric power plant has been carried out in U.S.A and Japan. Not long before, it seems that a PAFC power plant will be the one of commercial power plant [4]. Fig. 1 shows a simplified schematic diagram of phosphoric acid fuel cell.

The performance of PAFC is affected by the efficiencies of components such as electrodes, matrix, and electrolyte, etc., and by the operation conditions. These variables must be known to predict the performance of stack and heat and mass transfer in the stack. So, interrelated equations of heat and mass transfer and electrochemistry must be solved. Since it is impossible to solve these equations analytically, numerical methods were applied [5].

For the best efficiency of a fuel cell, the performance and endurance of each component must be guaranteed. After the stack is

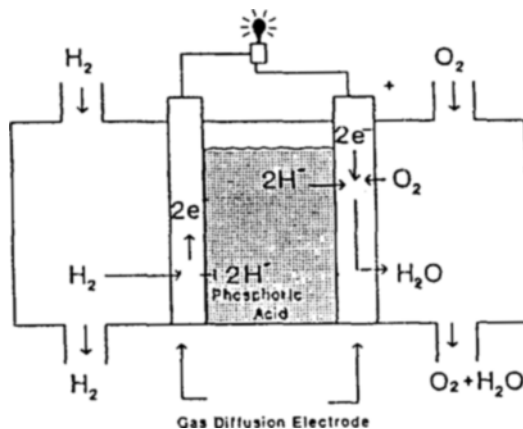


Fig. 1. Schematic diagram of a phosphoric acid fuel cell.

made, variables concerned with the hardware are regarded fixed, and optimal conditions for operation are obtained through the variation of operational conditions. There are flow rate, temperature, and output of stack as operating variables. PAFC must be operated at temperature between 180-200°C owing to the characteristics of electrolyte and endurance of electrode. For the cell efficiency increases with temperature, the cell must be operated at high temperature as long as the endurance of its components is not impaired. The inner part of stack shows 3-dimensional temperature distribution that can be affected by the design variables and operation variables. It is important that temperature distribution should be uniform to obtain maximum performance of fuel cell.

SYSTEM DESCRIPTION

The objective system of this study is 30-plate phosphoric acid fuel cell stack which has DIGAS (DItributed GAS) cooling system and external manifolds. DIGAS cooling is relatively simple and

[†]To whom all correspondences should be addressed.

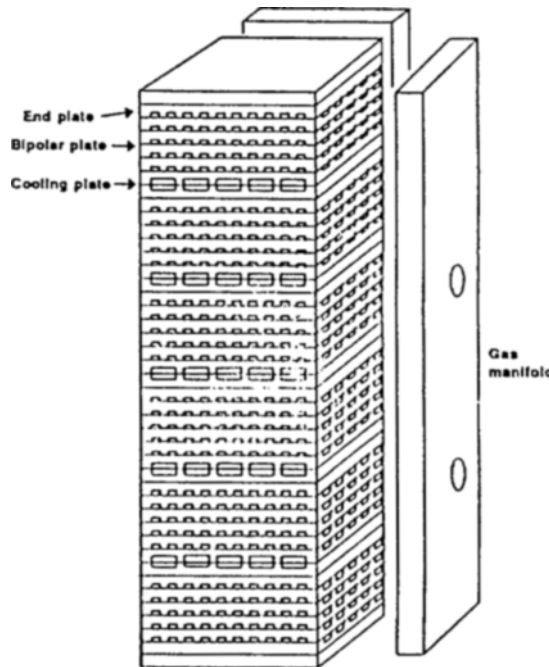


Fig. 2. Schematic diagram of 30-plate stack.

reliable. Since the cooling plates are similar in design to bipolar cell plates, no special cooling gas manifolds are required. The air stream is supplied into air manifold and split into two separate streams. One is a reactant stream and the other is a coolant stream. The reactant air is distributed to the cathode via channelled bipolar plates made from a graphite-resin composite material that has a thermal conductivity of about 85 Kcal hr⁻¹m⁻¹K⁻¹. The coolant part of the air flows through channels in cooling plates interspersed in stack after every fifth cell plate. Fig. 2 shows a simplified schematic diagram of 30-plate stack.

The size of plates is 19 cm × 19 cm and thickness is 8 mm. The depth and width of cell plate channels are 1.5 mm and those of cooling plate channels are 3 mm and 6 mm. And the effective cell area is about 225 cm². Since original electrode area is 19 cm × 15 cm, only the overlapped area was considered and edge sealed areas were neglected.

The temperatures of inlet and outlet gas and a few selected plates are measured by thermocouples. The thermocouples are located in the inside of bipolar plates and in reactant gas channels which are blocked by sealant. Some measured values are used for the basic data of calculation.

MODEL FORMULATION

The activation overpotential and the resistance overpotential generated in electrode cause a voltage loss. The voltage loss increases temperature of a cell because it is converted into heat. So, the heat must be removed by a coolant. We removed the heat by diffusing reacting gases into reacting plates and cooling gas into cooling plates, which is called DIGAS cooling, in 30-plate stack.

5 Electrode plates and 1 cooling plate are repeating unit of 30-plate stack. Thus, the temperature profile and current density distributions in the unit could be assumed vertically symmetric forms around the center cell plate of unit. Two and half electrode

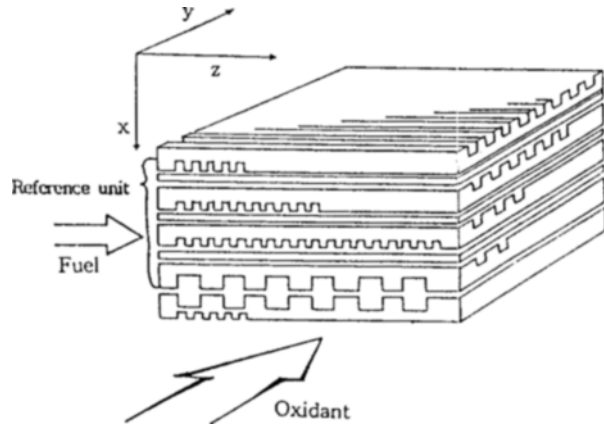


Fig. 3. Geometry of reference unit.

plates and half cooling plate were selected as a reference unit for the analysis. These are shown in Fig. 3.

The heat transfer in a stack is expressed by the partial differential equations [6-8]. The terms of the first equation express heat conduction in plates, heat transferred by gases and heat generated. This equation is an integrated form of second order partial differential equation in direction of stacking (x), from 0 to plate thickness (t).

$$t \left(K_y \frac{\partial^2 T}{\partial y^2} + K_z \frac{\partial^2 T}{\partial z^2} \right) + K_x \left(\frac{\partial T}{\partial x} \right)_i - K_x \left(\frac{\partial T}{\partial x} \right)_o - \left(\frac{M_p C_p}{P_p} \right) \left(\frac{dT_p}{dy} \right) - \left(\frac{M_F C_F}{P_F} \right) \left(\frac{dT_F}{dz} \right) = -(E - V) I \quad (1)$$

The convective heat transfers between plates and gases are expressed by following equations.

$$\begin{aligned} M_p C_p \frac{dT_p}{dy} &= h_p S_p (T - T_p) \\ M_F C_F \frac{dT_F}{dz} &= h_F S_F (T - T_F) \\ M_C C_C \frac{dT_C}{dy} &= h_C S_C (T - T_C) \end{aligned} \quad (2)$$

The heat transfer coefficient is an external function of Nusselt number and a hydraulic diameter. If the assumption is pertinent that a flow of each gas is an incompressible laminar flow, Nusselt number is given in terms of the widths and depths of channels [8].

$$\begin{aligned} h &= \text{Nu} \cdot k/w \\ \text{Nu} &= 3.61 + 4.63(1 - w_D/w_w) \end{aligned} \quad (3)$$

The operation voltage (V) is expressed as the difference between theoretical potential and overpotentials.

$$V = E - \eta_o - \eta_i \quad (4)$$

The theoretical potential (E) is given by Nernst equation. This is a function of temperature and partial pressures of gases. The value of theoretical potential is about 1.2 V at the operation conditions.

$$E = 1.261 - 0.00025T + \frac{RT}{nF} \ln \frac{P_{H_2} P_{O_2}^{1/2}}{P_{H_20}} \quad (5)$$

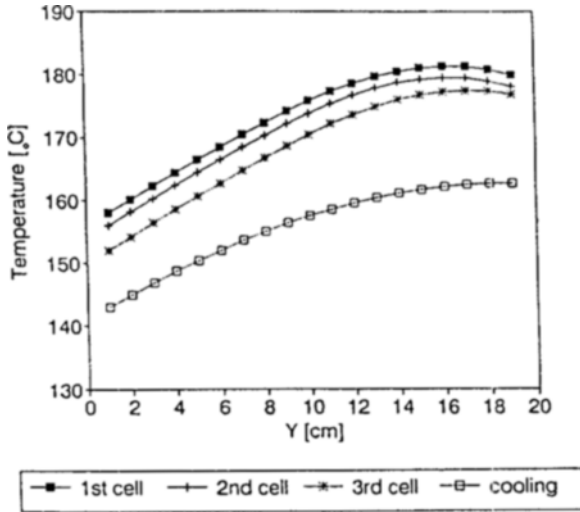


Fig. 4. Result of 2-dimensional calculation.

The resistance overpotential is given as a function of current density and the internal resistance of cell.

$$\eta_r = I \cdot r(T)$$

$$r(T) = r_0 \cdot \exp \left[3650 \left(\frac{1}{T} - \frac{1}{450} \right) \right] \quad (6)$$

The activation overpotential can be expressed as a function of temperature, current density and the constants related to catalyst.

$$\eta_a = \frac{RT}{2\alpha F} \ln \frac{I}{i_a S_a C_a C_u} \quad (7)$$

The resistance and the activation overpotential are functions of temperature and current density. The resistance overpotential has a tendency to increase proportionally as the output current increases. So, in case of maintaining the output voltage constant, we can calculate the temperatures and the current densities in cell corresponding to the partial pressures of gases.

NUMERICAL CALCULATION PROCEDURE

The partial pressures and compositions of each gas stream vary in the direction of flows and affect current generation and temperature distribution. Especially reactant gas and coolant have much effect on temperature distribution. So, 2-dimensional analysis was performed in the direction of reactant gas flow and vertical direction with current generation equation which has a term proportional to partial pressure of reactant gas. One result of 2-dimensional analysis using ERC (Energy Research Corporation)'s experimental data as the boundary values is shown in Fig. 4. This result is similar to ERC's experimental results in many respects [3]. The results of 2 dimensional analysis were used as initial temperature profile in 3-dimensional analysis for raising accuracy and making initial guess easy. And current density profiles were calculated by equation of V-I characteristics at initial local temperatures. Then calculated local current densities were used for calculation of temperature profiles in heat transfer equations. For these calculations several conditions were assumed.

1. The surroundings of a stack are insulated.
2. The repeating unit of electrode plates and cooling plate is

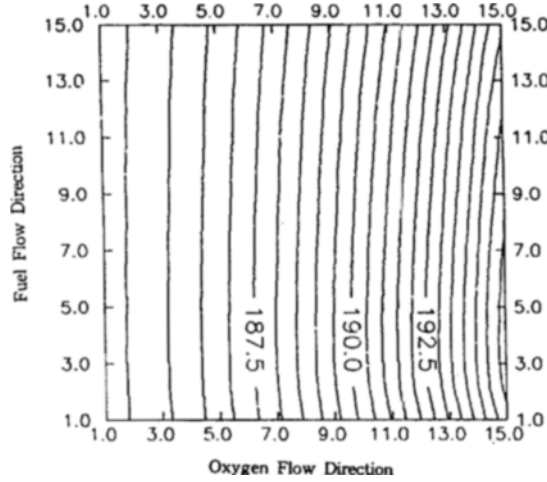


Fig. 5. Temperature distribution in the first cell plate.
(V=0.7 V, H₂: 10 l/min, O₂: 60 l/min)

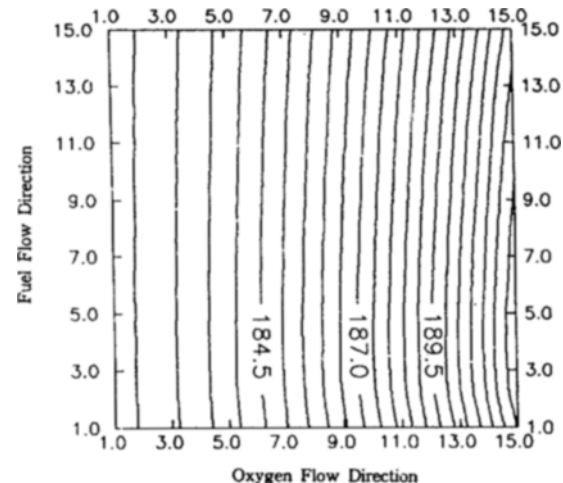


Fig. 6. Temperature distribution in the second cell plate.
(V=0.7 V, H₂: 10 l/min, O₂: 60 l/min)

analyzed.

3. The operating voltage of a cell is maintained constant.
4. All flows of gases in cell can be regarded as the laminar flows of ideal gases.
5. The current densities and the quantity of heat generations have a uniform distribution during operation.
6. The heat conductivities of the electrode and the cooling plates are constant.
7. All heats are transferred by the conductions in the plates and the convections between gases and plates.

RESULTS AND DISCUSSION

The following figures are the typical results of 3-dimensional analysis. They display temperature profiles of each plates and current distribution of the first cell plate in overlapped area of electrodes (15 cm × 15 cm). Fig. 5 shows temperature distribution profile of plate 1 at operation voltage of 0.7 V. The flow rate of hydrogen gas is 10 l/min and that of oxygen gas is 60 l/min (include coolant). The temperature difference in the direction of hydrogen gas flow (Z) is very small because heat capacity of hy-

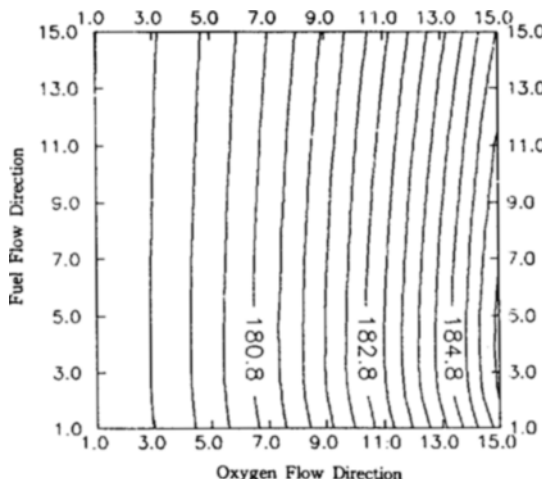


Fig. 7. Temperature distribution in the third cell plate.
($V = 0.7$ V, H_2 : 10 l/min, O_2 : 60 l/min)

Table 1. Comparison of calculated values with measured values			
T(x,y,z)	Measured	Calculated	Difference
T(1,5,5)	187	186.7	0.3
T(1,8,8)	189	188.3	0.7
T(1,12,5)	193	191.8	1.2
T(1,12,12)	192	190.7	1.3
T(2,5,5)	185	183.8	1.2
T(2,8,8)	187	185.7	1.3
T(2,12,5)	189	189.0	0.0
T(2,12,12)	189	188.7	0.3

hydrogen gas is relatively small and hydrogen is consumed along the gas flow direction. But there are some temperature drops near the inlet part of direction Z. In the direction of oxygen gas flow (Y), the temperature of plate increased more and more rapidly because the increasement of oxygen gas and cooling gas temperature decreased heat removal effect of convective heat transfer. Fig. 6 and Fig. 7 show the temperature distributions of cell plate 2 and 3. The temperature distribution profiles are shown as almost flat lines. Maximum temperature difference in a plate is about 10°C. This results correspond with measured temperatures. In Table 1, measured data and calculated data are compared [9].

Fig. 8 shows the current density distribution profile in the first plate at the same condition. The current density is higher near the hydrogen gas inlet area and increase in oxygen gas flow direction because current generation is affected by cell temperatures and partial pressures of gases. In this case, the partial pressures of hydrogen gas and cell temperatures are important factors. Fig. 9 shows the current density distribution at the condition of isothermal plate. It only affected by partial pressures of gases.

The partial pressure of oxygen gas has relatively little effect on current distribution because the current density is affected by temperature of cell plate and the partial pressure differences of oxygen gas are relatively small. To increase the utilization ratio of oxygen, the flow rate of oxygen should be decreased. But oxygen flow rate cannot be decreased below some minimum point because the coolant is fed simultaneously with reactant gas in DIGAS cooling system.

Fig. 10 shows current density distribution calculated with the

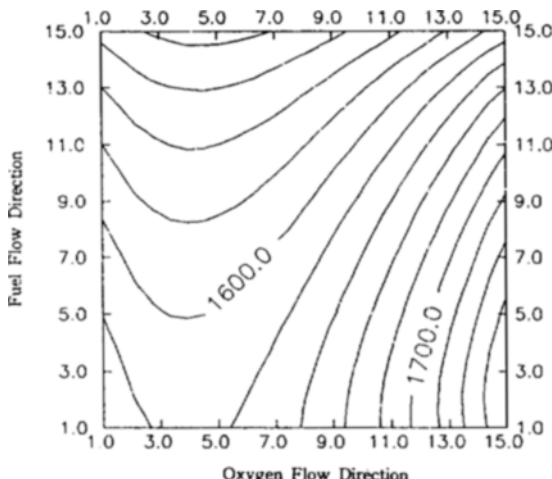


Fig. 8. Current density distribution in the first cell plate.
 $(V=0.7 \text{ V}, \text{H}_2: 10 \text{ l/min}, \text{O}_2: 60 \text{ l/min})$

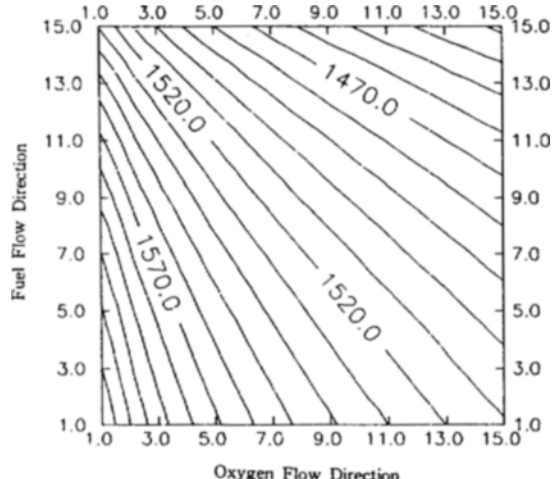


Fig. 9. Current density distribution in the first cell plate with using average temperature (at 170°C).
(V = 0.7 V, H₂: 10 l/min, O₂: 60 l/min)

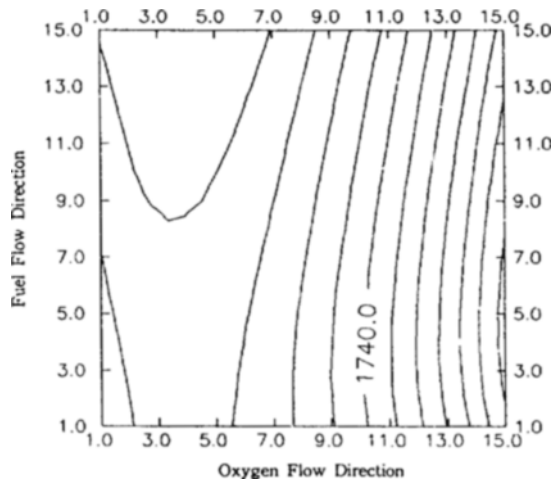


Fig. 10. Current density distribution in the first cell plate with increased hydrogen supply.
($V=0.7$ V, H_2 : 20 l/min, O_2 : 60 l/min)

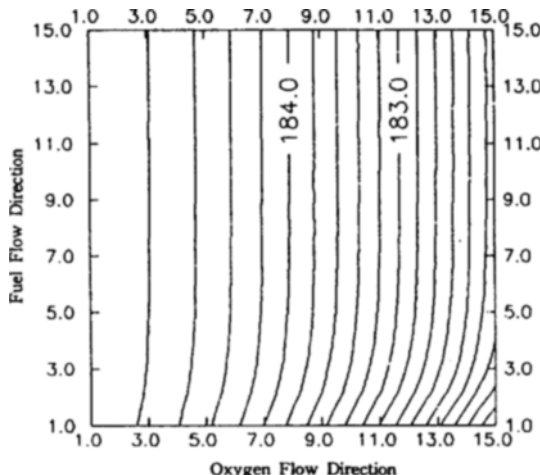


Fig. 11. Temperature distribution in the first cell plate with using average values of current densities.
($V=0.7$ V, H_2 : 10 l/min, O_2 : 60 l/min)

increased hydrogen gas flow rate. The current density distribution profile is more flat and the current densities are increased. However, the utilization ratio of fuel decreases as the fuel flow rate increases. Because the utilization ratio of fuel is directly related to economical efficiency of fuel cell, the flow rate of fuel should be maintained at the optimum value.

The calculation results in this study show relatively flat and well distributed profiles of temperatures and current densities. The maximum temperature deviation from the experimentally measured values was 1.3°C. In some previous studies [6, 10], the current densities were calculated at average temperature or temperatures at average current density. But in this study, the results of 2-dimensional calculation were used as the initial values and every calculation were performed with the local values. For the comparison, temperature profile in first cell plate was showed in Fig. 11 which was calculated by using average values of temperature and current density. Its temperature profile was very different from results of previous calculation. The temperature of cell plate decreased in direction of oxygen flow and difference of temperatures in plate was less than 3°C.

CONCLUSION

The 30-plate DIGAS cooling PAFC stack was analyzed and modelled by combining the elecrochemical equations and mass and heat transfer equations. 2-Dimensional calculations were performed and those results used as the initial values for 3-dimensional calculations. The temperature and the current density profiles are calculated by using the local values of temperatures and current densities and compared by experimentally measured values. The results of comparison show that the 3-dimensional model and calculation of this study can be used to predict the temperature and current density distribution in stack and the effects of some operation variables.

ACKNOWLEDGEMENT

The authors gratefully acknowledge the financial support of Honam Oil Refinery Co.

NOMENCLATURE

C	: heat capacity [J/mol]
C_L	: adhesive density of catalyst [kg/m ²]
C_u	: utilization ratio of catalyst
E	: theoretical potential [V]
F	: Faraday's constant [96500]
I	: current density [A/m ²]
K	: conductivity of plate [J/m·s·K]
N_u	: Nusselt's number
P	: partial pressure [atm]
P_F, P_p	: pitch of cell plate channel [m]
R	: gas constant [8.314 J/mol·K]
S	: perimeter of gas channel [m]
S_a	: effective surface area of electrode [m ² /kg]
T	: temperature [K]
V	: operation voltage [V]
h	: convective heat transfer coefficient [J/m·s·K]
i_0	: exchange current density [A/m ²]
k	: conductive heat transfer coefficient of gases [J/m·s·K]
n	: number of electrons concerned with reaction
r_0	: internal resistance of stack at 450 K [Ω]
t	: thickness of bipolar plate [m]
w	: hydraulic diameter [m]
w_D	: depth of channel [m]
w_w	: width of channel [m]

Greek Letters

α	: transfer coefficient of charge
η_a	: activation overpotential
η_r	: resistant overpotential

Subscripts

C	: coolant
F	: fuel
H_2	: hydrogen
H_2O	: water
O_2	: oxygen
P	: process gas (oxidant)
x, y, z	: direction of coordination

REFERENCES

1. Berger, C.: "Handbook of Fuel Cell Technology", Prentice-Hall (1968).
2. Kinoshita, K., McLarnon, F. R. and Cairns, E. J.: "Fuel Cell A Hand Book", Lawrence Berkeley Laboratory (1988).
3. Appleby, A. J. and Foulkes, F. R.: "Fuel Cell Handbook", Van Nostrand Reinhold (1989).
4. Bockris, J. O. M. and Srinivasan, S.: "Fuel Cell: Their Electrochemistry", McGraw Hill Inc. (1969).
5. Hirschenhofer, J. H.: "Commercial Fuel Cell Technology Status", 26th IECEC, 3, 531 (1991).
6. Alkasab, K. A. and Lu, C. Y.: "Phosphoric Acid Fuel Cell Power Plant Performance Model and Computer Program", NASA CR-174638 (1984).
7. Hoover, D. O.: "Cell and Stack Design Alternatives", first qly. Rept. of Westinghouse Corp. to NASA, Lewis, Contract No. Et-78-C-03-2031, Jan. (1979).
8. Alkasab, K. A.: *International Journal of Energy System*, 5, 1

(1985).

9. Sung, J. Y., et al.: "Development of Technology for Manufacturing Phosphoric Acid Fuel Cell Stack", Final Report, MOTIE 932I101-608DP1, Ministry of Trade, Industry and Energy, Seoul, Korea (1994).

10. Maru, H. C., Chi, C., Patel, D. and Burns, D.: "Heat Transfer in Phosphoric Acid Fuel Cell Stacks", 13th IECEC, 724 (1978).